acquired the resistance against Ozagrel. We analyzed partial genomic sequences of the drug-resistant HCVs by the direct sequencing method. We found that 68 base substitutions, 10 of which were accompanied with amino acid substitution, were present in such HCV genomes, compared with those in the mice untreated with the drug (Supplementary Figure 15). This indicated that the HCV proliferating in the chimeric mouse treated with Ozagrel included a large number of base substitutions in the genome. Further study of such drug-resistant HCV, for example, the reverse genetic analysis using a recombinant HCV system, will help to reveal the molecular mechanisms of the medicinal effects of this drug and the infectious HCV production. Furthermore, these results show the need to find the optimum dose of TXAS inhibitor for effective therapy and to use this drug as one option with different action mechanisms for multidrug therapy.

Supplementary Material

Note: To access the supplementary material accompanying this article, visit the online version of *Gastroenterology* at www.gastrojournal.org, and at http://dx.doi.org/10.1053/j.gastro.2013.05.014.

References

1. Wasley A, Alter MJ. Epidemiology of hepatitis C: geographic differences and temporal trends. Semin Liver Dis 2000;20:1–16.
2. Younossi Z, Kallman J, Kincaid J. The effects of HCV infection and management on health-related quality of life. Hepatology 2007; 45:806–816.
3. Fried MW, Shiffman ML, Reddy KR, et al. Peginterferon alfa-2a plus ribavirin for chronic hepatitis C virus infection. N Engl J Med 2002; 347:975–982.
4. Gao M, Nettles RE, Belema M, et al. Chemical genetics strategy identifies an HCV NS5A inhibitor with a potent clinical effect. Nature 2010;465:96–100.
5. Chayama K, Takahashi S, Toyota J, et al. Dual therapy with the nonstructural protein 5A inhibitor, daclatasvir, and the nonstructural protein 3 protease inhibitor, asunaprevir, in hepatitis C virus genotype 1b-infected null responders. Hepatology 2012; 55:742–748.
6. Lin C, Kwong AD, Perni RB. Discovery and development of VX-950, a novel, covalent, and reversible inhibitor of hepatitis C virus NS3.4A serine protease. Infect Disord Drug Targets 2006;6:3–16.
7. Sarrazin C, Zeuzem S. Resistance to direct antiviral agents in patients with hepatitis C virus infection. Gastroenterology 2010; 138:447–462.
8. **Wakita T, Pietschmann T,** Kato T, et al. Production of infectious hepatitis C virus in tissue culture from a cloned viral genome. Nat Med 2005;11:791–796.
9. Lindenbach BD, Evans MJ, Syder AJ, et al. Complete replication of hepatitis C virus in cell culture. Science 2005;309:623–626.
10. **Zhong J, Gastaminza P,** Cheng G, et al. Robust hepatitis C virus infection in vitro. Proc Natl Acad Sci U S A 2005;102:9294–9299.
11. Miyanari Y, Atsuzawa K, Usuda N, et al. The lipid droplet is an important organelle for hepatitis C virus production. Nat Cell Biol 2007;9:1089–1097.
12. Aly HH, Watashi K, Hijikata M, et al. Serum-derived hepatitis C virus infectivity in interferon regulatory factor-7-suppressed human primary hepatocytes. J Hepatol 2007;46:26–36.
13. Aly HH, Qi Y, Atsuzawa K, et al. Strain-dependent viral dynamics and virus-cell interactions in a novel in vitro system supporting the life cycle of blood-borne hepatitis C virus. Hepatology 2009; 50:689–696.
14. Aly HH, Shimotohno K, Hijikata M. 3D cultured immortalized human hepatocytes useful to develop drugs for blood-borne HCV. Biochem Biophys Res Commun 2009;379:330–334.
15. Chockalingam K, Simeon RL, Rice CM, et al. A cell protection screen reveals potent inhibitors of multiple stages of the hepatitis C virus life cycle. Proc Natl Acad Sci U S A 2010;107:3764–3769.
16. Gastaminza P, Whitten-Bauer C, Chisari FV. Unbiased probing of the entire hepatitis C virus life cycle identifies clinical compounds that target multiple aspects of the infection. Proc Natl Acad Sci U S A 2010;107:291–296.
17. Bos CL, Richel DJ, Ritsema T, et al. Prostanoids and prostanoid receptors in signal transduction. Int J Biochem Cell Biol 2004; 36:1187–1205.
18. Little P, Skouteris GG, Ord MG, et al. Serum from partially hepatectomized rats induces primary hepatocytes to enter S phase: a role for prostaglandins? J Cell Sci 1988;91:549–553.
19. Rudnick DA, Perlmutter DH, Muglia LJ. Prostaglandins are required for CREB activation and cellular proliferation during liver regeneration. Proc Natl Acad Sci U S A 2001;98:8885–8890.
20. Waris G, Siddiqui A. Hepatitis C virus stimulates the expression of cyclooxygenase-2 via oxidative stress: role of prostaglandin E2 in RNA replication. J Virol 2005;79:9725–9734.
21. Tateno C, Yoshizane Y, Saito N, et al. Near completely humanized liver in mice shows human-type metabolic responses to drugs. Am J Pathol 2004;165:901–912.
22. Kushima Y, Wakita T, Hijikata M. A disulfide-bonded dimer of the core protein of hepatitis C virus is important for virus-like particle production. J Virol 2010;84:9118–9127.
23. Gastaminza P, Kapadia SB, Chisari FV. Differential biophysical properties of infectious intracellular and secreted hepatitis C virus particles. J Virol 2006;80:11074–11081.
24. Kamiya N, Iwao E, Hiraga N, et al. Practical evaluation of a mouse with chimeric human liver model for hepatitis C virus infection using an NS3-4A protease inhibitor. J Gen Virol 2010; 91:1668–1677.
25. Flavahan NA. Balancing prostanoid activity in the human vascular system. Trends Pharmacol Sci 2007;28:106–110.
26. Bartenschlager R, Penin F, Lohmann V, et al. Assembly of infectious hepatitis C virus particles. Trends Microbiol 2011;19:95–103.
27. Andre P, Komurian-Pradel F, Deforges S, et al. Characterization of low- and very-low-density hepatitis C virus RNA-containing particles. J Virol 2002;76:6919–6928.
28. Nielsen SU, Bassendine MF, Burt AD, et al. Association between hepatitis C virus and very-low-density lipoprotein (VLDL)/LDL analyzed in iodixanol density gradients. J Virol 2006; 80:2418–2428.
29. Aizaki H, Morikawa K, Fukasawa M, et al. Critical role of virion-associated cholesterol and sphingolipid in hepatitis C virus infection. J Virol 2008;82:5715–5724.
30. Shimizu Y, Hishiki T, Sugiyama K, et al. Lipoprotein lipase and hepatic triglyceride lipase reduce the infectivity of hepatitis C virus (HCV) through their catalytic activities on HCV-associated lipoproteins. Virology 2010;407:152–159.
31. Gryglewski RJ. Prostacyclin among prostanoids. Pharmacol Rep 2008;60:3–11.
32. Forman BM, Tontonoz P, Chen J, et al. 15-Deoxy-delta 12, 14-prostaglandin J2 is a ligand for the adipocyte determination factor PPAR gamma. Cell 1995;83:803–812.
33. Gupta RA, Tan J, Krause WF, et al. Prostacyclin-mediated activation of peroxisome proliferator-activated receptor delta in colorectal cancer. Proc Natl Acad Sci U S A 2000;97:13275–13280.
34. Pawlotsky JM, Chevaliez S, McHutchison JG. The hepatitis C virus life cycle as a target for new antiviral therapies. Gastroenterology 2007; 132:1979–1998.

35. Wohnsland A, Hofmann WP, Sarrazin C. Viral determinants of resistance to treatment in patients with hepatitis C. Clin Microbiol Rev 2007;20:23–38.

Author names in bold designate shared co-first authorship.

Received August 11, 2012. Accepted May 13, 2013.

Reprint requests

Address requests for reprints to: Makoto Hijikata, PhD, Laboratory of Human Tumor Viruses, Department of Viral Oncology, Institute for Virus Research, Kyoto University, 53, Kawaharacho, Shogoin, Sakyoku, Kyoto 606-8507, Japan. e-mail: mhijikat@virus.kyoto-u.ac.jp; fax: (81) 75-751-3998.

Acknowledgments

The authors thank Dr Michinori Kohara (Tokyo Metropolitan Institute of Medical Science, Tokyo, Japan) for providing anti-hepatitis C virus core antibody; Toyobo, Co (Osaka, Japan) for providing hollow fibers; Toray, Co (Tokyo, Japan) for providing Beraprost; and Dr Masayoshi Fukasawa (National Institute of Infectious Disease, Tokyo, Japan) for helpful discussion.

Present address of H.H.A.: Department of Virology 2, National Institute of Infectious Disease, Tokyo, Japan.

Transcript Profiling: The microarray data in this study was named "HuSE2, 2Dvs3D," and was registered in ArrayExpress. Accession number: E-MTAB-1491.

Nucleic acid sequences: Sequencing data in this study were named "BankIt1626925 Seq1" and "BankIt1626925 Seq3", and registered with GenBank. Accession numbers: KF006982 and KF006984, respectively.

Conflicts of interest

The authors disclose no conflicts.

Funding

Supported by grants-in-aid from the Ministry of Health, Labour and Welfare of Japan.

Supplementary Materials and Methods

Preparation of Subcellular Fraction and Protein Detection With Western Blotting

Subcellular fractions of HuS-E/2 cells and patient's tissues were prepared with the ProteoExtract Subcellular proteome Extraction Kit (Millipore, Billerica, MA) according to the manufacturer's protocol. Five micrograms of total protein of each fraction or whole-cell lysate of each cell was analyzed by Western blotting. Western blotting was performed as described previously.[1]

Collection of Total RNA and Cell Lysate From HCV-Infected Patients' Tissue

Total RNA from patients' tissue was collected with RNeasy mini (Qiagen, Hilden, Germany). In brief, frozen tissues were homogenized in lysis buffer with a Power Masher (Nippi, Tokyo, Japan). Homogenized samples were used for RNA purification according to the manufacturer's protocol. Cell lysate from tissues were collected with RIPA buffer (Thermo Scientific, Waltham, MA) or the ProteoExtract Subcellular proteome Extraction Kit according to the manufacturer's protocol.

cAMP Reporter Assay

Huh-7–derived and HuS-E/2 cells were transfected with pCRE-Luc (Agilent Technologies, Santa Clara, CA) using Fugene6 (Roche) and Effectene (Qiagen), respectively, essentially according to the manufacturers' protocols. Six hours and 2 days post-transfection of Huh-7–derived and HuS-E/2 cells, respectively, the culture medium was replaced with fresh medium containing one of the reagents. One and 3 day(s) post-transfection of Huh-7–derived and HuS-E/2 cells, respectively, luciferase activity in the cells was measured using a luciferase activity detection reagent (Promega, Madison, WI) and a Lumat LB 9507 luminometer (EG&G Berthold, Bad Wildbad, Germany).

Calcium Ion Quantification

HEK293, Huh-7–derived, and HuS-E/2 cells were treated with the calcium ionosphere A23187 (Sigma-Aldrich) and the TP agonist U-46619 for 1 day. Calcium ion concentrations were quantified using a calcium assay kit (Cayman Chemical) according to the manufacturer's protocols.

Actin Polymerization Assay

Activation of actin polymerization via TP was measured with fluorescein isothiocyanate–phalloidin (Sigma-Aldrich). After culture in lipid-free fresh medium, cells were stimulated with 10 μmol/L U46619 containing medium for 30, 60, and 180 seconds. Then, samples were stained with 10 μg/mL fluorescein isothiocyanate phalloidin, Fluorescent intensity at 520 nm was measured.

Fatty Acid Analysis

Fatty acid analysis of HCV-infected Huh-7.5 cells treated with or without Ozagrel was performed by Toray Research Center, Inc, Tokyo, Japan using gas chromatography. Total fatty acid samples were extracted from the cells according to the Bligh-Dyer[2] method.

Secondary Infection Experiments in Chimeric Mice Transplanted Human Hepatocytes

The chimeric mice were inoculated intravenously with patient serum including 1.0×10^5 genome titer of bbHCV (genotype 1b) as the first infection. Ozagrel was administered orally twice each day (300 μg/day) 1 week after the inoculation. The serum samples from those mice were collected at 5 weeks after starting the drug treatments, and used as inocula in the secondary infection experiment. Naive chimeric mice were inoculated with the collected chimeric mice serum including 1.0×10^5 genome titer of HCV. Administration of Ozagrel was started simultaneously. HCV-RNA levels in the blood of the chimeric mice at 1, 2, and 3 weeks after infection in secondary infection experiments were evaluated by qRT-PCR.

Determination of Nucleotide Sequence of HCV Genome After Treatment With Ozagrel

Chimeric mice were inoculated secondarily with sera from HCV-infected chimeric mice with or without Ozagrel treatment. Sera of these chimeric mice treated with or without Ozagrel were collected 5 weeks after the inoculation and the start of the treatment. HCV genome sequences of these samples were determined by the direct sequencing method according to the protocol described previously.[3] HCV genomic sequences obtained from sera of mice with 2 different types of treatment were compared with each other. Mice with 2 different types of treatments were as follows: first, mice inoculated secondarily with sera from the first chimeric mouse without treatment were not treated with the drug (BankIt1626925 Seq3 in GenBank). Second, mice inoculated secondarily with sera from the first chimeric mouse with treatment were treated with the drug (BankIt1626925 Seq1 in GenBank). These sequencing data were registered with GenBank (http://www.ncbi.nlm.nih.gov/genbank/).

Supplementary References

1. Kushima Y, Wakita T, Hijikata M. A disulfide-bonded dimer of the core protein of hepatitis C virus is important for virus-like particle production. J Virol 2010;84:9118–9127.
2. Bligh EG, Dyer WJ. A rapid method of total lipid extraction and purification. Can J Biochem Physiol 1959;37:911–917.
3. Kimura T, Imamura M, Hiraga N, et al. Establishment of an infectious genotype 1b hepatitis C virus clone in human hepatocyte chimeric mice. J Gen Virol 2008;89:2108–2113.

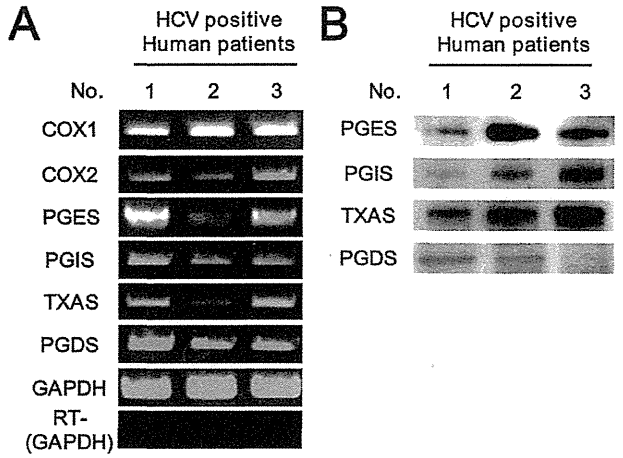

Supplementary Figure 1. Protein and mRNA levels of PG synthases in HCV-infected patient tissue. (*A* and *B*) mRNA expression and protein levels of PG synthases in HCV-infected patient tissue. Representative results from 2 independent experiments are shown.

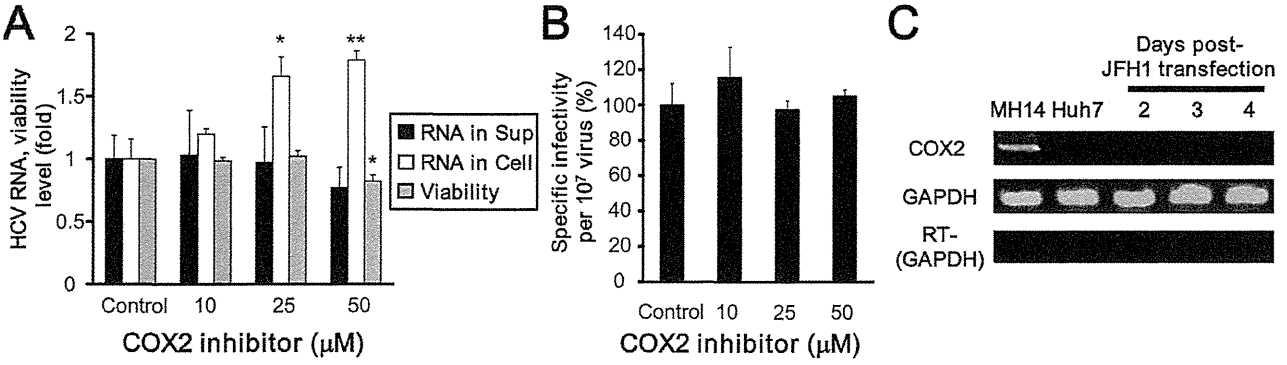

Supplementary Figure 2. Effects of COX2 inhibitor 1 on infectious HCV production. (*A*) Effects of COX2 inhibitor 1 on HCV-RNA levels in the HCVcc-producing cell-culture system. Levels of HCV RNA in medium (*black bars*) and cells (*white bars*) treated with or without COX2 inhibitor 1 were assessed with qRT-PCRs and plotted as amounts relative to results observed with control cells (control). Mean cell viability ± SD for each sample condition also is plotted (*gray bars*). (*B*) Effects of COX2 inhibitor 1 on the infectivity of HCVcc produced using the cell-culture system. (*C*) Expression of COX2 mRNA in MH14 (positive control), Huh-7, and JFH1-transfected Huh-7 cells. *Differs from control, $P < .01$; **differs from control, $P < .001$.

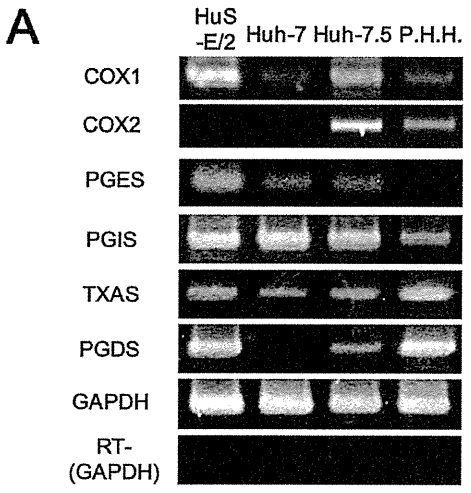

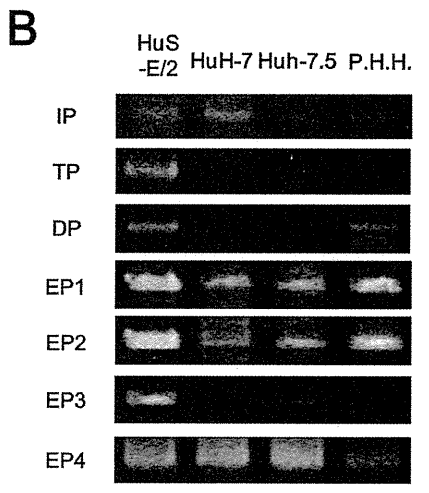

Supplementary Figure 3. Expression of PG synthase and PG-receptor mRNA in immortalized and primary hepatocyte cell lines. (*A* and *B*) mRNA expression levels of various PG synthases and PG receptors in HuS-E/2 cells, Huh-7 cells, Huh-7.5 cells, and primary human hepatocytes were analyzed in RT-PCRs. Representative results from 2 independent experiments are shown.

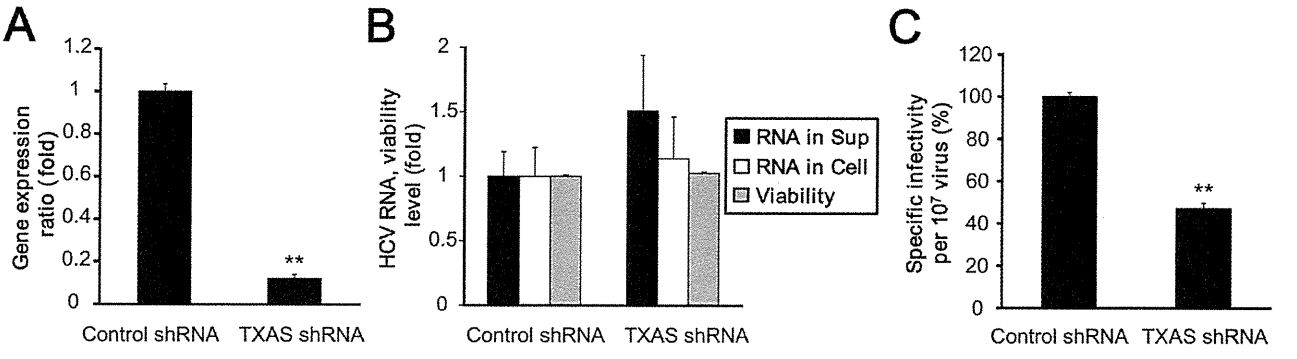

Supplementary Figure 4. Effects of short hairpin RNA (shRNA)-mediated knockdown of TXAS mRNA levels on infectious HCV production. (*A*) Knockdown of TXAS mRNA levels using shRNA. (*B*) Effects of TXAS-specific shRNA on HCV-RNA levels in the HCVcc-producing cell culture system. Levels of HCV RNA in medium (*black bars*) and cells (*white bars*) treated with control or TXAS-specific shRNA were assessed with qRT-PCRs and plotted as amounts relative to results observed with control shRNA–treated cells (control). Mean cell viability ± SD for each sample condition also is plotted (*gray bars*). (*C*) Effects of TXAS-specific shRNA on the infectivity of HCVcc produced using the cell-culture system. **Differs from control, $P < .001$.

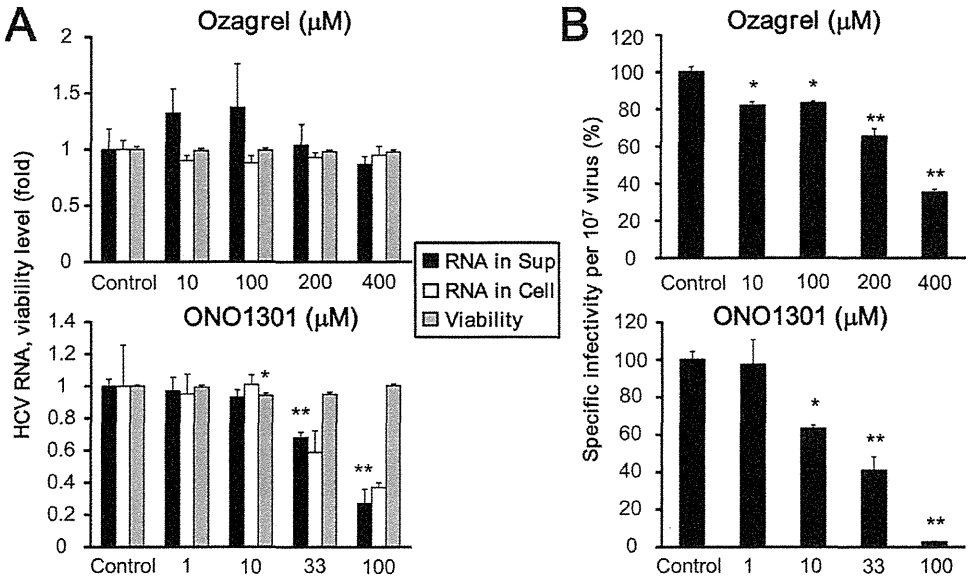

Supplementary Figure 5. Effects of Ozagrel and ONO1301 on the infectivity of HCVcc produced from J6/JFH1-transfected Huh-7.5 cells. (*A*) Effects of Ozagrel (*upper panel*) and ONO1301 (*lower panel*) on HCV-RNA levels in HCVcc-producing cell cultures. Levels of HCV RNA in the medium (*black bars*) and cells (*white bars*) treated with Ozagrel or ONO1301 cells were assessed in qRT-PCRs and plotted as the amount relative to results from untreated cells (control). Mean cell viability ± SD for each sample condition also is plotted (*gray bars*). (*B*) Effects of Ozagrel (*upper panel*) and ONO1301 (*lower panel*) on the infectivity of HCVcc produced in the cell-culture system. *Differs from control, $P < .01$; **differs from control, $P < .001$.

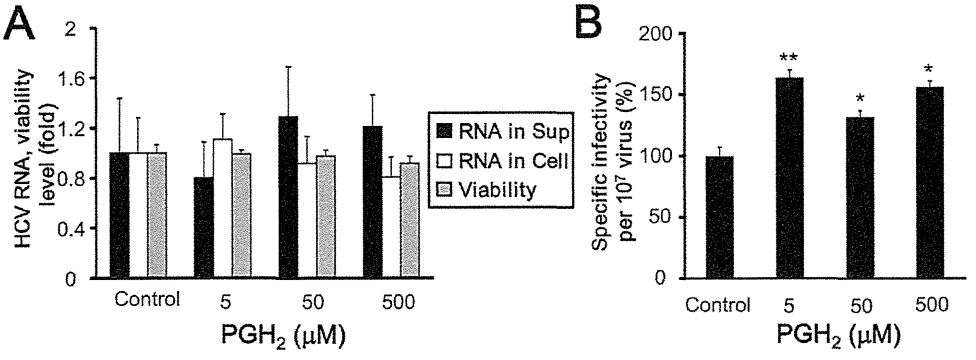

Supplementary Figure 6. Effects of PGH_2 on infectious HCV production. (*A*) Effects of PGH_2 on HCV-RNA levels in the HCVcc-producing cell-culture system. Levels of HCV RNA in medium (*black bars*) and cells (*white bars*) treated with or without PGH_2 were assessed with qRT-PCRs and plotted as amounts relative to results observed with control cells (control). Mean cell viability ± SD for each sample condition also is plotted (*gray bars*). (*B*) Effects of PGH_2 on the infectivity of HCVcc produced using the cell culture system. *Differs from control, $P < .01$; **differs from control, $P < .001$.

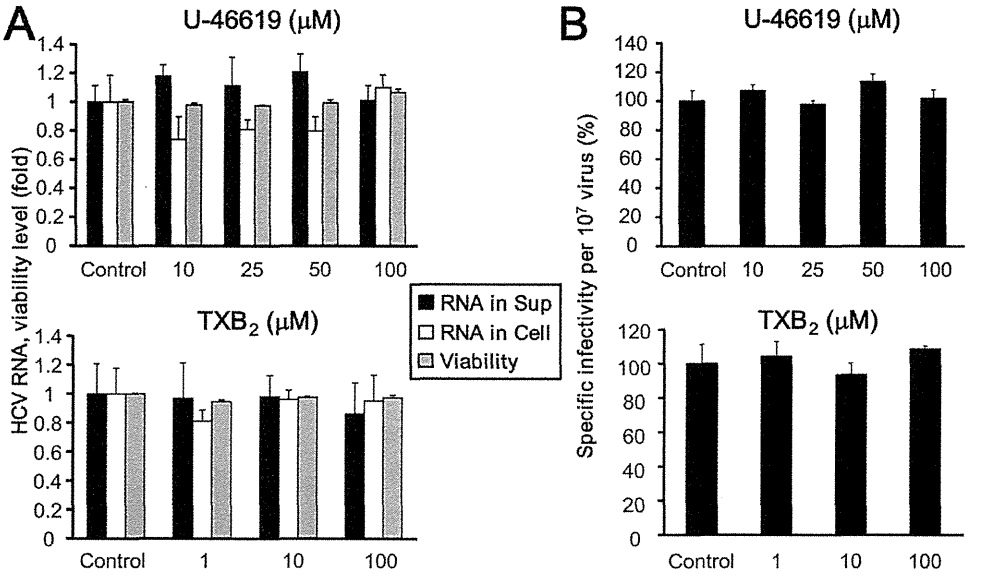

Supplementary Figure 7. Effects of U-46619 and TXB_2 on infectious HCV production. (*A*) Effects of U-46619 (*upper panel*) and TXB_2 (*lower panel*) on HCV-RNA levels in HCVcc-producing cell cultures. Levels of HCV RNA in the medium (*black bars*) and cells (*white bars*) treated with U-46619 or TXB_2 were assessed in qRT-PCRs and plotted as the amount relative to results observed with untreated cells (control). Mean cell viability ± SD for each sample condition also is plotted (*gray bars*). (*B*) Effects of U-46619 (*upper panel*) and TXB_2 (lower panel) on the infectivity of HCVcc produced in the cell-culture system were assessed.

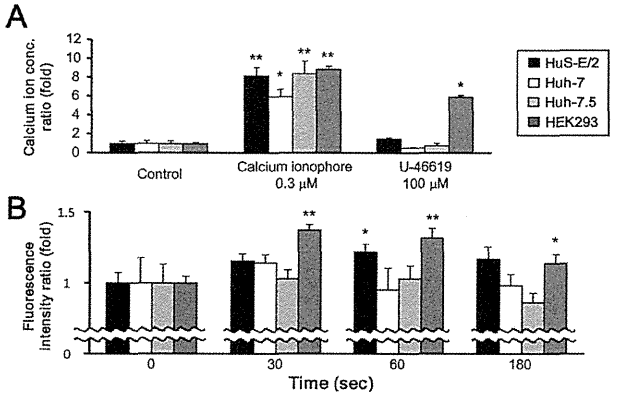

Supplementary Figure 8. Effects of U-46619 on HuS-E/2, Huh-7, Huh-7.5, and HEK293 cell lines via TP. (*A*) Concentrations of intracellular calcium ions were measured in HuS-E/2 (*black bars*), Huh-7 (*white bars*), Huh-7.5 (*gray bars*), and HEK293 (*dark gray bars*) cells treated with or without a calcium ionophore or U-46619. Calcium ion concentrations relative to those in mock-treated cells (control) were determined from triplicate wells in 2 independent experiments and are shown as means ± SD. (*B*) Actin polymerization after U-46619 treatment was measured with fluorescein isothiocyanate (FITC)-labeled phalloidin. *Differs from control, $P < .01$; **differs from control, $P < .001$.

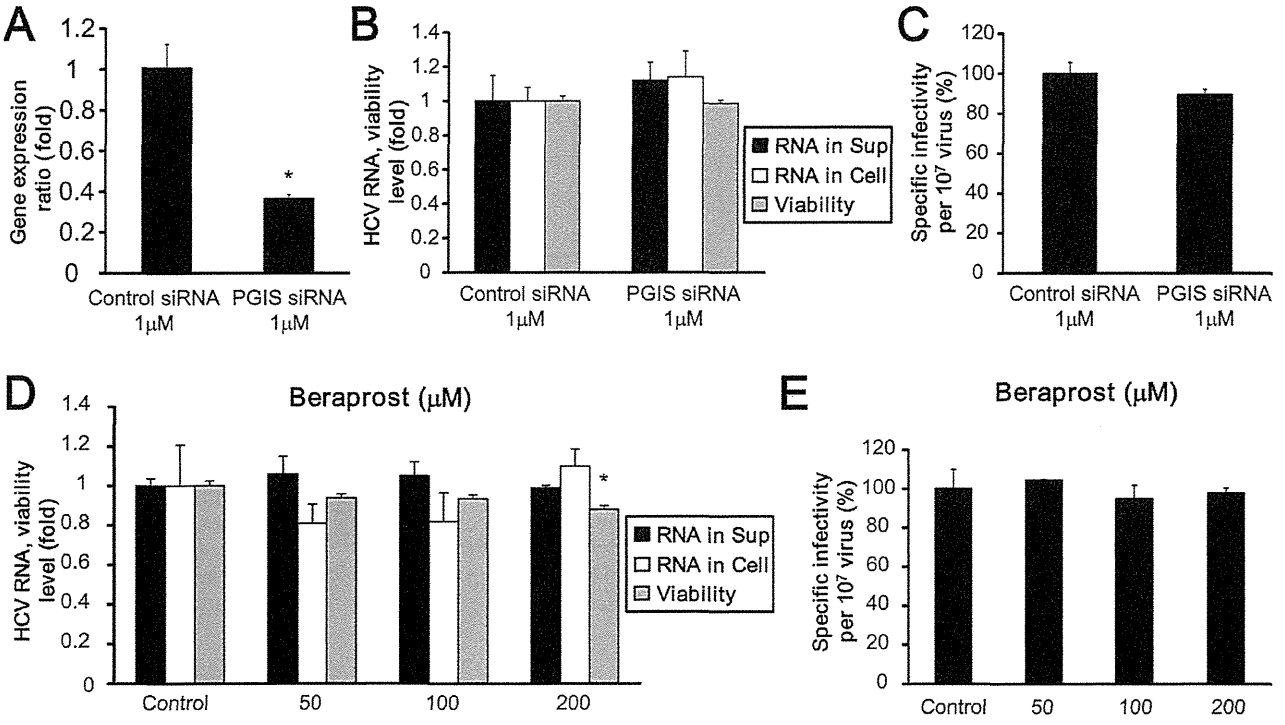

Supplementary Figure 9. Effects of PGI_2 on infectious HCV production. (*A*) siRNA-mediated knockdown of PGIS expression. (*B*) Effects of PGIS-specific siRNA on HCV-RNA levels in HCVcc-producing cell cultures. Levels of HCV RNA in medium (*black bars*) and cells (*white bars*) treated with control or PGIS-specific siRNA were assessed in qRT-PCR and are plotted as amounts relative to results obtained with control siRNA–treated cells (control). Mean cell viability ± SD for each sample condition also is plotted (*gray bars*). (*C*) Effects of PGIS-specific siRNA on the infectivity of HCVcc produced in the cell-culture system. (*D*) Effects of Beraprost on HCV-RNA levels in HCVcc-producing cell cultures. Levels of HCV RNA in medium (*black bars*) and HCVcc-producing Huh-7 cells (*white bars*) treated with Beraprost were assessed in qRT-PCRs and plotted as amounts relative to results obtained with untreated cells (control). Mean cell viability ± SD for each sample condition also is plotted (*gray bars*). (*E*) Effects of Beraprost on the infectivity of HCVcc in culture medium from HCVcc-producing cell cultures were assessed. *Differs from control, $P < .01$.

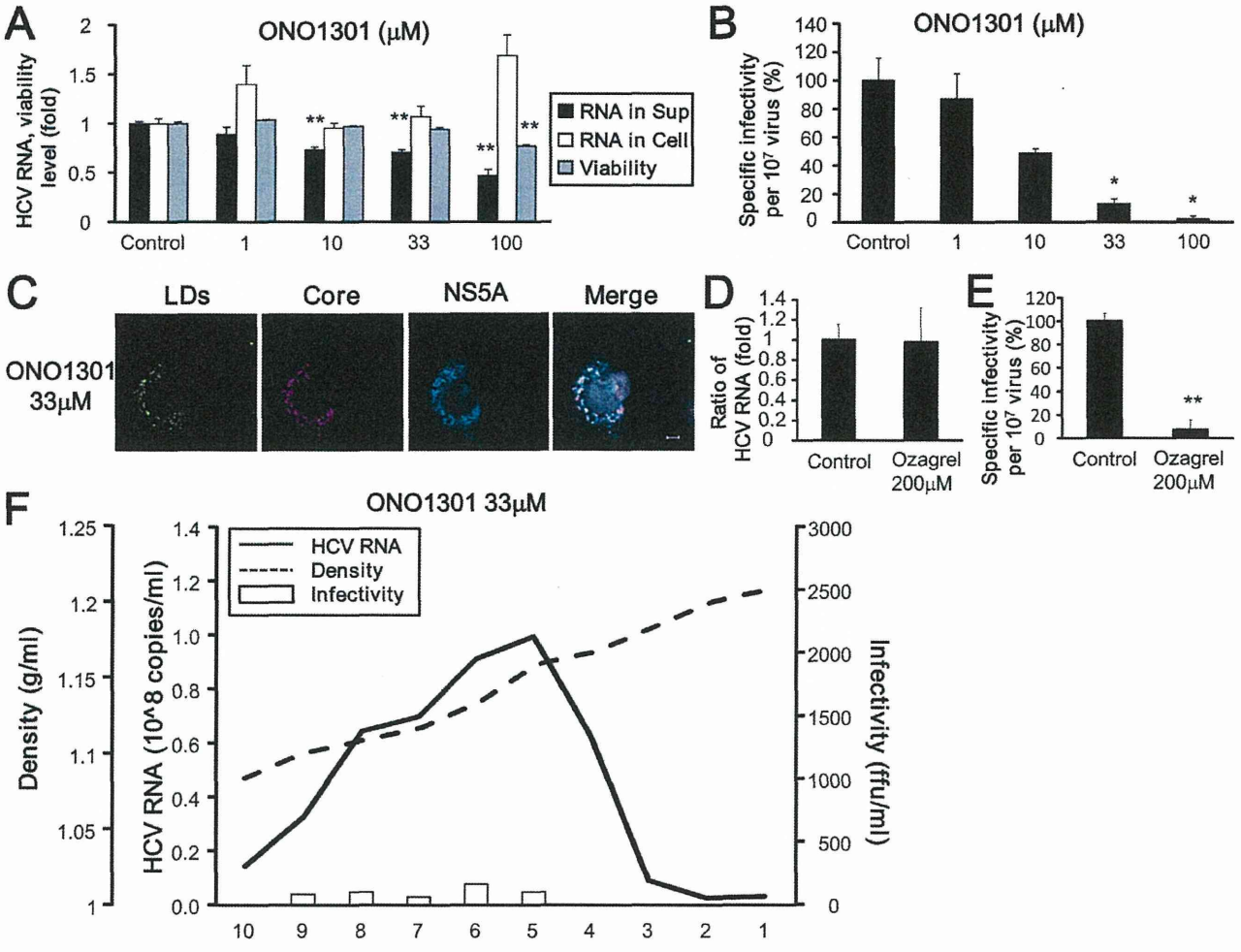

Supplementary Figure 10. Effects of ONO1301 on HCV lifecycle. (*A*) Levels of HCV RNA in medium (*black bars*) and cells (*white bars*) treated with or without ONO1301 were assessed. Mean cell viability ± SD for each sample condition also is plotted (*gray bars*). (*B*) The infectivity of HCVcc in culture medium from HCVcc-producing cell cultures treated with or without ONO1301 was assessed. (*C*) Subcellular locations of HCV core and NS5A proteins around LDs in the presence of ONO1301. Scale bars, 5 μm. (*D* and *E*) Levels and infectivity of intracellular HCV obtained from the cells treated with ONO1301. (*F*) Buoyant density of HCVcc obtained using cells treated with ONO1301. HCV RNA (*solid line*), fraction density (*dotted line*), and HCV infectivity (*white bars*) in each fraction collected by ultracentrifugation. *Differs from control, $P < .01$; **differs from control, $P < .001$.

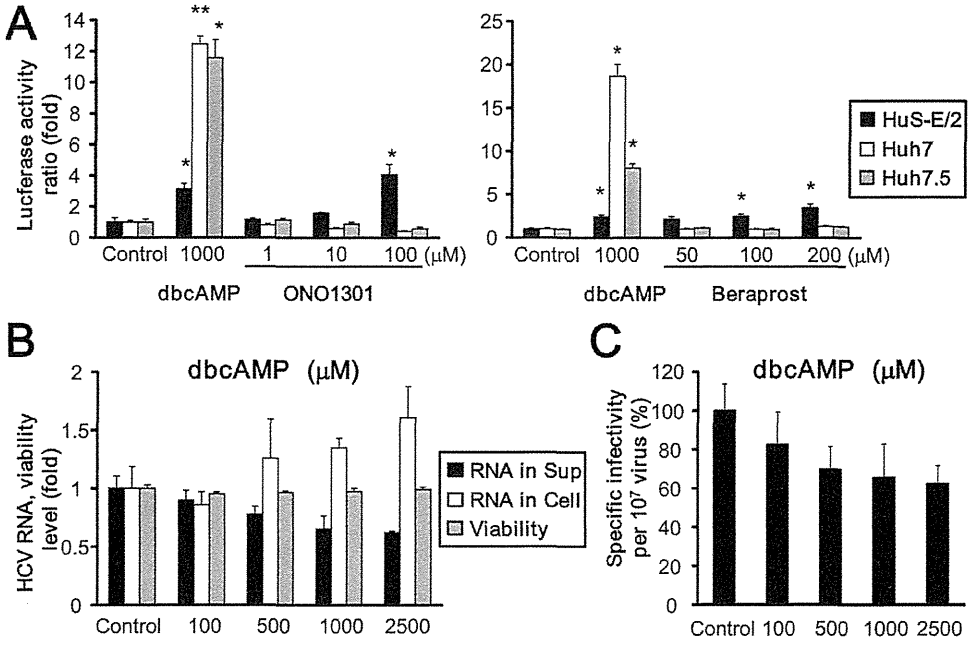

Supplementary Figure 11. Effects of dibutyryl cAMP (dbcAMP) on cell cultures producing JFH1 HCVcc. (*A*) HuS-E/2 (*black bars*), Huh-7 (*white bars*), and Huh-7.5 (*gray bars*) cells were transfected with CRE-Luc plasmid. Then, the luciferase activity in each sample was measured. Values were obtained from quadruplicate wells in 2 independent experiments and are shown as means ± SD. (*B*) Effects of dbcAMP on HCV-RNA levels in HCVcc-producing cell cultures. Levels of HCV RNA in medium (*black bars*) and cells treated with dbcAMP (*white bars*) were assessed in qRT-PCRs and plotted as amounts relative to results obtained with mock-treated cells (control). Mean cell viability ± SD for each sample condition also is plotted (*gray bars*). (*C*) Effects of dbcAMP on the infectivity of HCVcc produced using the cell-culture system. *Differs from control, $P < .01$; **differs from control, $P < .001$.

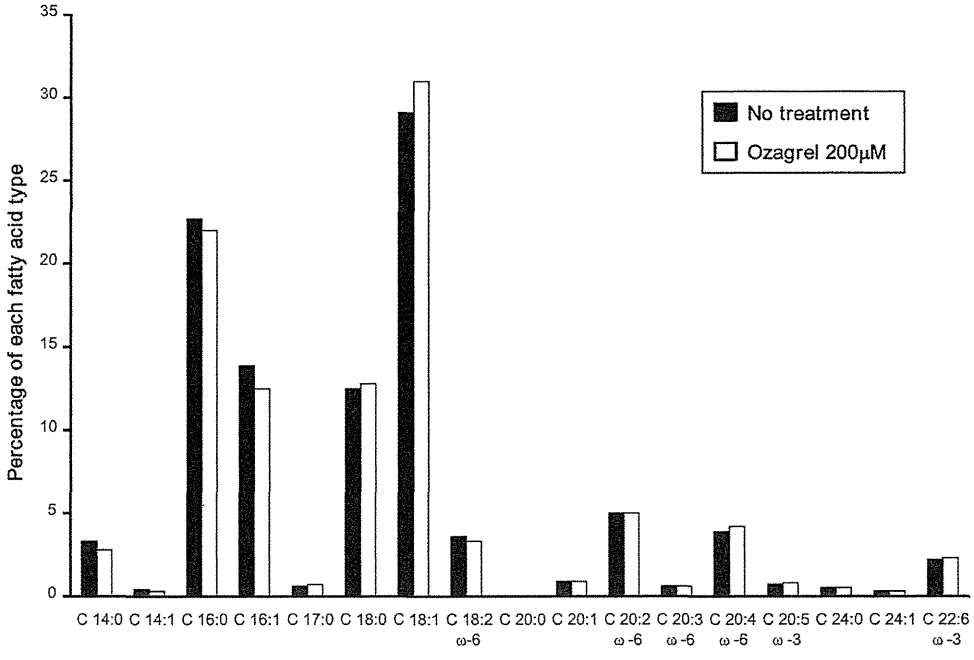

Supplementary Figure 12. Comparison of composition of fatty acids in HCV-infected Huh-7.5 cells with or without Ozagrel treatment.

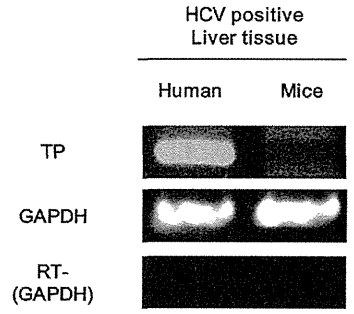

Supplementary Figure 13. Expression of TP mRNA in liver tissues from human patients and chimeric mice infected with HCV.

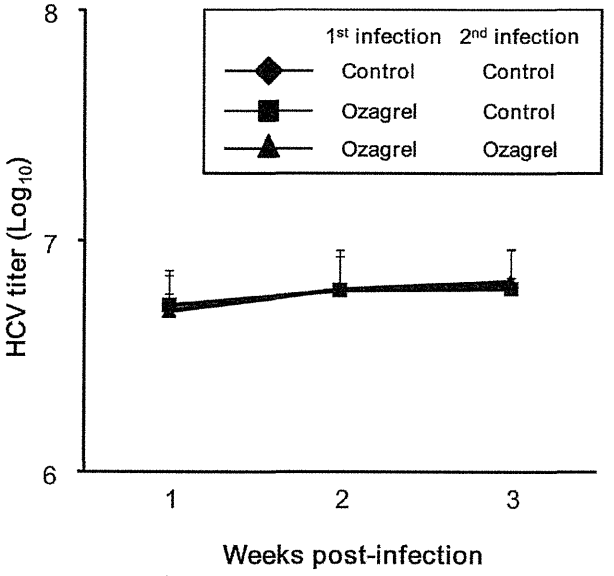

Supplementary Figure 14. Secondary infection of HCV derived from the chimeric mice model. Data are presented as means ± SD for 4 samples.

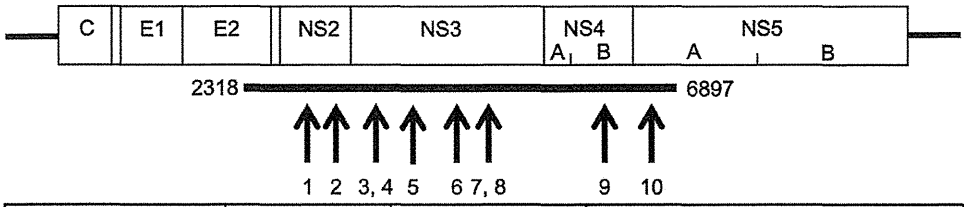

Supplementary Figure 15. Base substitutions in HCV genome collected from mice serum during a secondary infection. HCV genomic sequences from mice sera with Ozagrel treatment during primary and secondary infection was compared with those from mice without any treatment during both infection experiments. The region of obtained HCV genomic sequences is indicated (*thick bar*). The nucleotide positions of each base substitution are shown (*arrows*). Positions of base substitutions, and types of base substitution and amino acid replacement are listed in the *lower panel*.

Number of substitution point	Position of nucleotide	Single base substitution	Amino acid replacement
1	3192	A→G	Asparagine→Aspartic acid
2	3264	A→G	Isoleucine→Valine
3 4	3596 3597	T→A C→T	Phenylalanine→Tyrosine
5	3859	C→T	Serine→Leucine
6	4283	G→A	Methionine→Isoleucine
7 8	4437 4439	G→A T→C	Glycine→Serine
9	5886	G→A	Valine→Methionine
10	6747	G→A	Alanine→Threonine

Supplementary Table 1. Primer Sequences and Parameters in RT-PCR Experiments

Genes	Primer Sequence 5′-3′	Product size (bp)	Annealing Temperture	Cycle
COX1	F: GCAGCTGAGTGGCTATTTCC	324	60	32
	R: ATCTCCCGAGACTCCCTGAT			
COX2	F: GCAGTTGTTCCAGACAAGCA	383	60	35
	R: GGTCAATGGAAGCCTGTGAT			
PGES	F: GAAGAAGGCCTTTGCCAAC	200	62	35
	R: GGAAGACCAGGAAGTGCATC			
PGDS	F: AAGGCGGCGTTGTCCATGTGCAAGTC	400	55	40
	R: ATTGTTCCGTCATGCACTTATC			
PGIS	F: TCCTGGACCCACACTCCTAC	395	60	40
	R: GCGAAAGGTGTGGAAGACAT			
TXAS	F: TCTGCATCCCCAGACCTATC	374	60	40
	R: ATAGCCAGCGATGAGGAAGA			
GAPDH	F: ATGGGGAAGGTGAAGGTCGG	250	60	40
	R: TGGAGGGATCTCGCTCCTGG			
EP1	F: GGTATCATGGTGGTGTCGTG	324	60	40
	R: GGCCTCTGGTTGTGCTTAGA			
EP2	F: AGGAGAGGGGAAAGGGTGT	267	60	40
	R: TCTTAATGAAATCCGACAACAGAG			
EP3	F: GACAGTCACCTTTTCCTGCAAC	276	60	40
	R: AGGCGAACAGCTATTAAGAAGAAG			
EP4	F: CAGGACATCTGAGGGCTGAC	269	60	40
	R: GTAGAAGGTCGTCTCCTTCTGCTC			
DP	F: GCAACCTCTATGCGATGCAC	292	60	32
	R: GGGTCCACAATTGAAATCAC			
IP	F: AAGACTGGAGAGCCCAGACC	161	60	40
	R: CCACGAACATCAGGGTGCTG			
TP	F: CAGATGAGGTCTCTGAAGGTGTG	304	60	40
	R: CAGAGGAAGGTGAGGAAGGAG			

NOTE. RT-PCRs were performed as follows: 25–40 cycles of 95°C for 30 seconds, 55–62°C for 30 seconds, and 72°C for 1 minute.

Supplementary Table 2. Primer Sequences and Parameters in qRT-PCR Experiments

Genes	Primer Sequence 5′-3′	Product Size (bp)
COX1	F: TCCGGTTCTTGCTGTTCCTG	151
	R: TCACACTGGTAGCGGTCAAG	
PGES	F: CATCCTCTCCCTGGAAATCTCG	129
	R: CCGCTTCCTACTGTGACCC	
PGDS	F: CCTGTCCACCTTGCACAGTC	123
	R: TCATGCTTCGGTTCAGGACG	
PGIS	F: GCAGTGTCAAAAGTCGCCTG	83
	R: ACTCTCCAGCCATTTGCTCC	
TXAS	F: TTTGCTTGGTTGCCTGTTCC	99
	R: CCAGAGTGGTGGTCTTCCAG	
GAPDH	F: GACAGTCAGCCGCATCTTCT	104
	R: GCGCCCAATACGACCAAATC	

NOTE. qRT-PCRs were performed as follows: 40 cycles of 95°C for 5 seconds, 60°C for 34 seconds.

Biochemical and Biophysical Research Communications 430 (2013) 592–597

Contents lists available at SciVerse ScienceDirect

Biochemical and Biophysical Research Communications

journal homepage: www.elsevier.com/locate/ybbrc

PML tumor suppressor protein is required for HCV production

Misao Kuroki [a,b,c], Yasuo Ariumi [a,c,*], Makoto Hijikata [d], Masanori Ikeda [a], Hiromichi Dansako [a], Takaji Wakita [e], Kunitada Shimotohno [f], Nobuyuki Kato [a]

[a] Department of Tumor Virology, Okayama University Graduate School of Medicine, Dentistry, and Pharmaceutical Sciences, 2-5-1, Shikata-cho, Okayama 700-8558, Japan
[b] Research Fellow of the Japan Society for the Promotion of Science
[c] Center for AIDS Research, Kumamoto University, Kumamoto 860-0811, Japan
[d] Department of Viral Oncology, Institute for Virus Research, Kyoto University, Kyoto 606-8507, Japan
[e] Department of Virology II, National Institute of Infectious Diseases, Tokyo 162-8640, Japan
[f] Research Center for Hepatitis and Immunology, National Center for Global Health and Medicine, Ichikawa, Chiba 272-8516, Japan

ARTICLE INFO

Article history:
Received 8 November 2012
Available online 5 December 2012

Keywords:
Hepatitis C virus
PML
INI1
DDX5
Tumor suppressor
Lipid droplet

ABSTRACT

PML tumor suppressor protein, which forms discrete nuclear structures termed PML-nuclear bodies, has been associated with several cellular functions, including cell proliferation, apoptosis and antiviral defense. Recently, it was reported that the HCV core protein colocalizes with PML in PML-NBs and abrogates the PML function through interaction with PML. However, role(s) of PML in HCV life cycle is unknown. To test whether or not PML affects HCV life cycle, we examined the level of secreted HCV core and the infectivity of HCV in the culture supernatants as well as the level of HCV RNA in HuH-7-derived RSc cells, in which HCV-JFH1 can infect and efficiently replicate, stably expressing short hairpin RNA targeted to PML. In this context, the level of secreted HCV core and the infectivity in the supernatants from PML knockdown cells was remarkably reduced, whereas the level of HCV RNA in the PML knockdown cells was not significantly affected in spite of very effective knockdown of PML. In fact, we showed that PML is unrelated to HCV RNA replication using the subgenomic HCV-JFH1 replicon RNA, JRN/3-5B. Furthermore, the infectivity of HCV-like particle in the culture supernatants was significantly reduced in PML knockdown JRN/3-5B cells expressing core to NS2 coding region of HCV-JFH1 genome using the *trans*-packaging system. Finally, we also demonstrated that INI1 and DDX5, the PML-related proteins, are involved in HCV production. Taken together, these findings suggest that PML is required for HCV production.

1. Introduction

Hepatitis C virus (HCV) is the causative agent of chronic hepatitis, which progresses to liver cirrhosis and hepatocellular carcinoma. HCV is an enveloped virus with a positive single-stranded 9.6 kb RNA genome, which encodes a large polyprotein precursor of approximately 3000 amino acid residues. This polyprotein is cleaved by a combination of the host and viral proteases into at least 10 proteins in the following order: core, envelope 1 (E1), E2, p7, non-structural 2 (NS2), NS3, NS4A, NS4B, NS5A, and NS5B [1,2]. HCV core protein forms a viral capsid and is essential for infectious virion production. The core protein is targeted to lipid droplets. Recently, lipid droplets have been found to be involved in an important cytoplasmic organelle for HCV production [3].

In addition, HCV core has been reported to facilitate cellular transformation as well as development of hepatocellular carcinoma in HCV core-transgenic mice [4]. Interactions of core with tumor suppressor proteins such as p53 and DDX3 may lead to enhanced cellular proliferation [4]. Indeed, HCV core interacts with promyelocytic leukemia (PML) protein and inhibits the PML tumor suppressor pathway through interfering with the PML-mediated apoptosis-inducing function [5]. PML forms discrete nuclear structures termed PML-nuclear bodies (PML-NBs) and associates with several cellular functions, including cell proliferation, apoptosis and antiviral defense [6,7]. In acute promyelocytic leukemia (APL) patient, the PML gene is fused with the retinoic acid receptor-α (RARα) gene, thus resulting in expression of an oncogenic PML-RARα fusion protein [6,7]. Conversely, treatment of APL patient with arsenic trioxide leads to reformation of PML-NBs and results in disease remission [6,7], indicating that PML is a target of arsenic trioxide. Interestingly, we have recently demonstrated that arsenic trioxide strongly inhibited HCV infection and HCV RNA replication without cell toxicity [8]. However, the role of PML in HCV life cycle yet remains unclear. To investigate the possible involvement of PML in HCV life cycle, we examined the accumulation of HCV RNA as well as the release of HCV core into culture

* Corresponding author at: Center for AIDS Research, Kumamoto University, 2-2-1, Honjo, Kumamoto 860-0811, Japan. Fax: +81 96 373 6834.
E-mail address: ariumi@kumamoto-u.ac.jp (Y. Ariumi).

0006-291X/$ - see front matter Crown Copyright © 2012 Published by Elsevier Inc. All rights reserved.
http://dx.doi.org/10.1016/j.bbrc.2012.11.108

supernatants from cells rendered defective for PML by RNA interference. The results provide evidence that PML is required for HCV production.

2. Materials and methods

2.1. Cell culture

293FT cells were cultured in Dulbecco's modified Eagle's medium (DMEM; Invitrogen, Carlsbad, CA, USA) supplemented with 10% fetal bovine serum (FBS). The three HuH-7-derived cell lines: RSc cured cells that cell culture-generated HCV-JFH1 (JFH1 strain of genotype 2a) [9] could infect and effectively replicate [10–13], OR6c cells is cured cells of OR6 cells harboring the genome-length HCV-O RNA with luciferase as a reporter [14] or OR6c JRN/3-5B cells harboring the subgenome HCV-JFH1 RNA with luciferase as a reporter were cultured in DMEM with 10% FBS as described previously [13].

2.2. RNA interference

Oligonucleotides with the following sense and antisense sequences were used for the cloning of short hairpin RNA (shRNA)-encoding sequences targeted to DDX5 in a lentiviral vector: 5′-GATCCCCCTCTAATGTGGAGTGCGACTTCAAGAGAGTCGCACTCCACA TTAGAGTTTTTGGAAA-3′ (sense), 5′-AGCTTTTCCAAAAACTCTAATGT GGAGTGCGACTCTCTTGAAGTCGCACTCCACATTAGAGGGG-3′ (antisense). The oligonucleotides above were annealed and subcloned into the *Bgl*II-*Hin*dIII site, downstream from an RNA polymerase III promoter of pSUPER [15], to generate pSUPER-DDX5i. To construct pLV-DDX5i, the *Bam*HI-*Sal*I fragments of the pSUPER-DDX5i were subcloned into the *Bam*HI-*Sal*I site of pRDI292, an HIV-1-derived self-inactivating lentiviral vector containing a puromycin resistance marker allowing for the selection of transduced cells [16]. We previously described pLV-PMLi [8] and pLV-INI1i [17], respectively.

2.3. Lentiviral vector production

The vesicular stomatitis virus (VSV)-G-pseudotyped HIV-1-based vector system has been described previously [18,19]. The lentiviral vector particles were produced by transient transfection of the second-generation packaging construct pCMV-ΔR8.91 [18,19] and the VSV-G-envelope-expressing plasmid pMDG2 as well as pLV-PMLi into 293FT cells with FuGene6 (Roche Diagnostics, Mannheim, Germany).

2.4. HCV infection experiments

The supernatants was collected from cell culture-generated HCV-JFH1-infected RSc cells at 5 days post-infection and stored at −80 °C after filtering through a 0.45 μm filter (Kurabo, Osaka, Japan) until use. For infection experiments with HCV-JFH1 virus or J6/JFH1 [20], RSc cells (5×10^4 cells/well) were plated onto 6-well plates and cultured for 24 h (hrs). We then infected the cells at a multiplicity of infection (MOI) of 0.05. The culture supernatants were collected at the indicated time post-infection and the levels of the core protein were determined by enzyme-linked immunosorbent assay (Mitsubishi Kagaku Bio-Clinical Laboratories, Tokyo, Japan). Total RNA was isolated from the infected cellular lysates using RNeasy mini kit (Qiagen, Hilden, Germany) for quantitative RT-PCR analysis of intracellular HCV RNA. The infectivity of HCV-JFH1 in the culture supernatants was determined by a focus-forming assay at 48 h post-infection.

2.5. Quantitative RT-PCR analysis

The quantitative RT-PCR analysis for HCV RNA was performed by real-time LightCycler PCR (Roche) as described previously [14]. We used the following forward and reverse primer sets for the real-time LightCycler PCR: PML, 5′-GAGGAGTTCCAGTTTCT GCG-3′ (forward), 5′-GCGCCTGGCAGATGGGGCAC-3′ (reverse); DDX5, 5′-ATGTCGGGTTATTCGAGTGA-3′ (forward), 5′-TTTCTCC CCAGGGTTTCCAA-3′ (reverse); INI1, 5′-ATGATGATGATGGCGCTG AG-3′ (forward), 5′-TCGGAACATACGGAGGTAGT-3′ (reverse); β-actin, 5′-TGACGGGGTCACCCACACTG-3′ (forward), 5′-AAGCTGTAG CCGCGCTCGGT-3′ (reverse); and HCV-JFH1, 5′-AGAGCCATAGTGGT CTGCGG-3′ (forward), 5′-CTTTCGCAACCCAACGCTAC-3′ (reverse).

2.6. Western blot analysis

Cells were lysed in buffer containing 50 mM Tris–HCl (pH 8.0), 150 mM NaCl, 4 mM EDTA, 1% Nonidet P-40, 0.1% sodium dodecyl sulfate (SDS), 1 mM dithiothreitol and 1 mM phenylmethylsulfonyl fluoride. Supernatants from these lysates were subjected to SDS–polyacrylamide gel electrophoresis, followed by immunoblot analysis using anti-HCV core (CP-9 and CP-11; Institute of Immunology, Tokyo, Japan) or anti-β-actin antibody (Sigma).

2.7. WST-1 assay

RSc or OR6c JRN/3-5B cells (1×10^3 cells/well) were plated onto 96-well plates and cultured. The cells were subjected to the WST-1 cell proliferation assay (Takara Bio, Otsu, Japan) according to the manufacturer's protocol. The absorbance was read using a microplate reader at 440 nm with a reference wavelength of 690 nm.

2.8. Renilla luciferase (RL) assay

OR6c JRN/3-5B cells (1.5×10^4 cells/well) were plated onto 24-well plates and cultured for 72 h, then, subjected to the RL assay according to the manufacturer's instructions (Promega, Madison, WI, USA). A lumat LB9507 luminometer (Berthold, Bad Wildbad, Germany) was used to detect RL activity.

2.9. RNA synthesis and transfection

Plasmid pJRN/3-5B was linearized by digestion with *Xba*I and was used for RNA synthesis with T7 MEGAscript (Ambion) as previously described [13]. *In vitro* transcribed RNA was transfected into OR6c cells by electroporation as described previously [14].

2.10. Immunofluorescence and confocal microscopic analysis

Cells were fixed in 3.6% formaldehyde in phosphate-buffered saline (PBS), permeabilized in 0.1% Nonidet P-40 in PBS at room temperature, and incubated with anti-PML antibody (PM001, MBL) and anti-HCV core at a 1:300 dilution in PBS containing 3% bovine serum albumin (BSA) at 37 °C for 30 min. They were then stained with anti-Cy3-conjugated anti-mouse antibody (Jackson ImmunoResearch, West Grove, PA) or Alexa Fluor 647-conjugated anti-rabbit antibody (Molecular Probes, Invitrogen) at a 1:300 dilution in PBS containing BSA at 37 °C for 30 min. Lipid droplets and nuclei were stained with BODIPY 493/503 (Molecular Probes, Invitrogen) and DAPI (4′, 6′-diamidino-2-phenylindole), respectively. Following extensive washing in PBS, the cells were mounted on slides using a mounting media of SlowFade Gold antifade reagent (Invitrogen) added to reduce fading. Samples were viewed under a confocal laser-scanning microscope (FV1000; Olympus, Tokyo, Japan).

3. Results

3.1. PML is involved in the propagation of HCV

To investigate the potential role(s) of PML in HCV life cycle, we first used lentiviral vector-mediated RNA interference to stably knockdown PML in HuH-7-derived RSc cured cells that HCV-JFH1 [9] could infect and effectively replicate [10–13]. Real-time RT-PCR analysis for PML demonstrated a very effective knockdown of PML in RSc cells transduced with lentiviral vector expressing shRNA targeted to PML (Fig. 1A). To test the cell toxicity of shRNA, we examined WST-1 assay. In spite of very effective knockdown of PML, we demonstrated that the shRNA targeted to PML did not affect the cell viabilities (Fig. 1B). We next examined the level of secreted HCV core and the infectivity of HCV in the culture supernatants as well as the level of HCV RNA in PML knockdown RSc cells 24, 48, or 72 h after HCV-JFH1 infection at an MOI of 0.05. The results showed that the level of HCV RNA in PML knockdown cells was not affected until 72 h post-infection (Fig. 1C), while the release of HCV core protein into the culture supernatants was significantly suppressed in PML knockdown cells at 48 or 72 h post-infection (Fig. 1D). Consistent with this finding, the infectivity of HCV in the culture supernatants was also significantly suppressed in the PML knockdown cells at 48 or 72 h post-infection (Fig. 1E). We also obtained similar results using siRNA specific for human PML (siGENOME SMRT pool M-006547-01-0005, Dharmacon, Thermo Fisher Scientific, Waltham, MA) (data not shown). These results suggested that PML is associated with propagation of HCV.

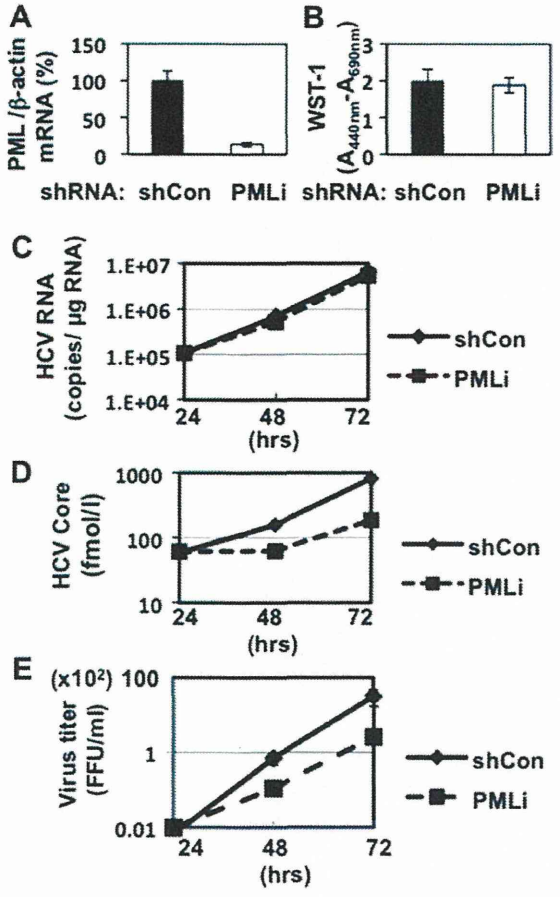

Fig. 1. PML is required for infectious HCV production. (A) Inhibition of PML mRNA expression by the shRNA-producing lentiviral vector. Real-time LightCycler RT-PCR for PML was performed as well as for β-actin mRNA. Each mRNA level was calculated relative to the level in RSc cells transduced with a control lentiviral vector (shCon) which was assigned as 100%. (B) WST-1 assay of the PML knockdown (PMLi) or the control (shCon) RSc cells. (C) The levels of intracellular genome-length HCV-JFH1 RNA in the PML knockdown or the control cells at 24, 48 or 72 h post-infection at an MOI of 0.05 were monitored by real-time LightCycler RT-PCR. (D) The levels of HCV core in the culture supernatants from the PML knockdown or the control RSc cells 24, 48 or 72 h after inoculation of HCV-JFH1 were determined by ELISA. (E) The infectivity of HCV in the culture supernatants was determined by a focus-forming assay at 48 h post-infection. All experiments were done in triplicate.

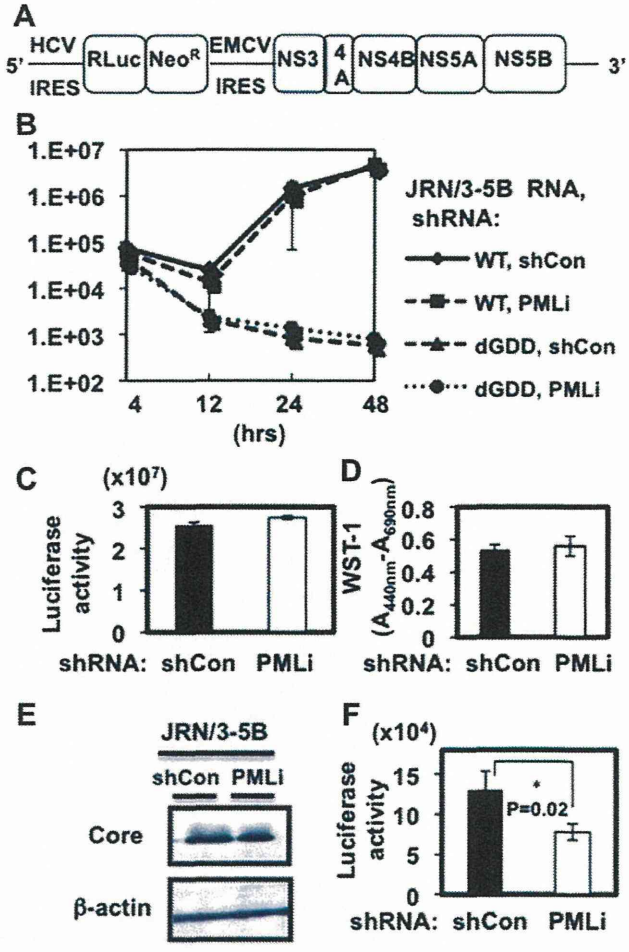

Fig. 2. PML is unrelated to the HCV RNA replication. Schematic gene organization of subgenomic JFH1 (JRN/3-5B) RNA encoding *Renilla* luciferase (RL) gene. *Renilla* luciferase gene (RLuc) is depicted as a box and is expressed as a fusion protein with Neo. (B) The transient replication of subgenomic HCV-JFH1 replicon in the PML knockdown (PMLi) or the control OR6c cells (shCon) after electroporation of *in vitro* transcribed JRN/3-5B RNA (10 μg) was monitored by RL assay at the indicated time. The results of *Renilla* luciferase activity are shown. dGDD indicates the deletion of the GDD motif in the NS5B polymerase, and the subgenomic HCV replicon with the deletion of GDD was used as a negative control. (C) The level of HCV RNA replication in PML knockdown (PMLi) or the control (shCon) OR6c JRN/3-5B cells was monitored by RL assay. The results shown are means from three independent experiments. (D) WST-1 assay of the PML knockdown or the control JRN/3-5B cells. (E) The level of HCV core protein in OR6c JRN/3-5B cells by expression of HCV core to NS2 coding region of HCV-JFH1 using mouse retroviral vector. pCX4bsr-JFH1-myc-C-NS2 and pMDG2 were cotransfected into Plat-E cells, mouse retroviral packaging cells. Mouse retroviral vector was obtained from their culture supernatants and transduced into OR6c JRN/3-5B PML knockdown or the control cells. The results of Western blot analysis of cellular lysates with anti-HCV core or an anti β-actin antibody are shown. (F) The level of HCV RNA replication in RSc cells 72 h after inoculation of HCV-like particles produced using *trans*-packaging system was monitored by RL assay. Asterisk indicates significant difference compared to the control. *$P = 0.02$.

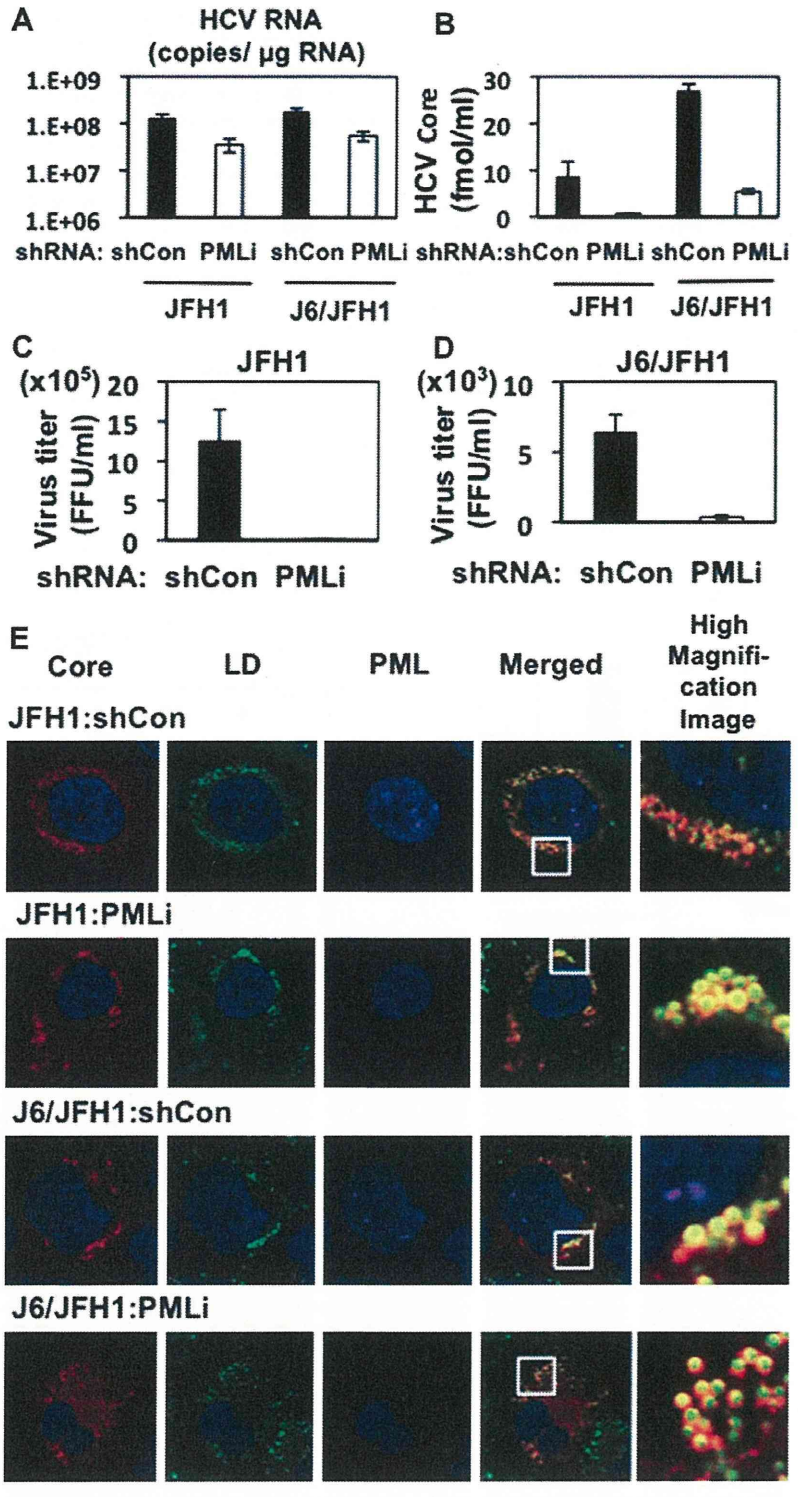

Fig. 3. PML is dispensable for the localization of HCV core to lipid droplet. (A) The levels of intracellular HCV RNA in PML knockdown or the control RSc cells 96 h after inoculation of HCV-JFH1 or HCV-J6/JFH1 were monitored by real-time LightCycler RT-PCR. Results from three independent experiments are shown (A–C). (B) The levels of HCV core in the culture supernatants from the PML knockdown RSc cells at 96 h post-infection were determined by ELISA. (C, D) The infectivity of HCV in the culture supernatants was determined by a focus-forming assay at 48 h post-infection. (E) HCV core localizes to lipid droplet (LD) in the PML knockdown (PMLi) or the control (shCon) cells after infection with either HCV-JFH1 or HCV-J6/JFH1. Cells were fixed 72 h post-infection and were then examined by confocal laser scanning microscopy.

3.2. PML is unrelated to HCV RNA replication

To examine whether or not PML is involved in HCV RNA replication, we used the subgenomic replicon RNA of HCV-JFH1, JRN/3-5B, encoding *Renilla* luciferase gene for monitoring the HCV RNA replication (Fig. 2A). *In vitro* transcribed JRN/3-5B RNA was transfected into the PML knockdown OR6c cells by electroporation and we examined the luciferase activity. Consequently, the

luciferase activity in the PML knockdown cells was similar to that of the control cells (Fig. 2B), indicating that shRNA targeted to PML could not affect the transient HCV RNA replication. As well, the level of HCV RNA in PML knockdown HuH-7-derived OR6c JRN/3-5B cells harboring the subgenomic replicon RNA of HCV-JFH1 and the cell growth was not affected (Fig. 2C and D), suggesting that PML is unrelated to the HCV RNA replication. To further confirm whether or not PML is involved in HCV production, we used *trans*-packaging system [21,22], that HCV subgenomic replicon was efficiently encapsidated into infectious virus-like particles by expression of HCV core to NS2 coding region. In fact, infectious HCV-like particles were produced and released into the culture medium from PML knockdown JRN/3-5B cells stably expressing core to NS2 coding region of HCV-JFH1 genome by mouse retroviral vector (Fig. 2E). We could monitor the HCV RNA replication by *Renilla* luciferase assay in target naïve RSc cells after the inoculation of infectious HCV-like particles. Consequently, the release of infectious HCV-like particles into the culture supernatants was significantly suppressed in PML knockdown cells at 72 h post-infection (Fig. 2F). Thus, we conclude that PML is associated with HCV production.

3.3. PML is required for the late step in the HCV-JFH1 life cycle

To avoid the possibility of specific finding when we only used HCV-JFH1, we examined another strain of HCV-J6JFH1 [20]. For this, we analyzed the level of HCV core and the infectivity in the culture supernatant as well as the level of HCV RNA in the PML knockdown RSc cells 96 h after inoculation of HCV-J6/JFH1. In this context, the level of HCV RNA in PML knockdown cells was only somewhat decreased (Fig. 3A), while the level of core and the infectivity in the culture supernatants was remarkably reduced (Fig. 3B–D), indicating that PML is required for infectious HCV-J6/JFH1 production as well as HCV-JFH1.

Since lipid droplets have been shown to be involved in an important cytoplasmic organelle for HCV production [3], we performed immunofluorescence and confocal microscopic analyses to determine whether or not HCV core misses localization into lipid droplets in the PML knockdown cells. We found that the core protein was targeted into lipid droplets even in PML knockdown RSc cells as well as in the control RSc cells after infection with either HCV-JFH1 or HCV-J6/JFH1 (Fig. 3E). This suggests that PML plays a role in the late step after the core is targeted into lipid droplet in the HCV life cycle. Importantly, HCV did not disrupt the formation of PML-NBs in response to HCV infection (Fig. 3E) unlike HIV-1 and other DNA viruses [6,7,23].

3.4. INI1 and DDX5, PML-related proteins, are involved in HCV production

Finally, we established the INI1 or DDX5, PML-related protein [23,24], knockdown RSc or OR6c JRN/3-5B cells by lentiviral vector expressing shRNA target to INI1 [17] or DDX5 to examine potential role of INI1 and DDX5 in HCV life cycle. Consequently, we found that the release of HCV core or the infectivity of HCV into the culture supernatants was significantly suppressed in the INI1 or DDX5 knockdown RSc cells 96 h after HCV-JFH1 infection, while the RNA replication in the knockdown cells was only somewhat decreased in spite of the very effective knockdown of INI1 or DDX5 mRNA without growth inhibition (Fig. 4A–F), suggesting that INI1 and DDX5 are involved in HCV life cycle. To confirm whether or not these proteins are involved in HCV RNA replication, we examined the luciferase assay in the INI1 or DDX5 knockdown OR6c JRN/3-5B cells. In this context, the shRNA target to INI1 or DDX5 did not affect the luciferase activity and the cell growth in these knockdown cells (Fig. 4G and H), suggesting that both INI1 and DDX5 are required for HCV production like PML.

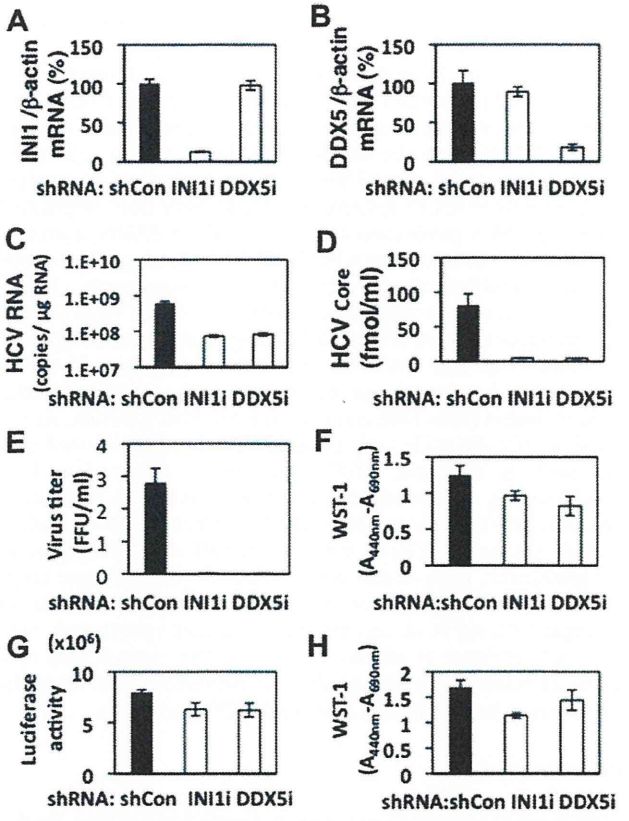

Fig. 4. INI1 and DDX5, PML-related proteins, are required for HCV production. (A, B) Inhibition of INI1 and DDX5 mRNA expressions by the shRNA-producing lentiviral vector. Real-time LightCycler RT-PCR for INI1 and DDX5 was performed as well as for β-actin mRNA in triplicate. Each mRNA level was calculated relative to the level in RSc cells transduced with a control lentiviral vector (Con) which was assigned as 100%. (C) The levels of intracellular genome-length HCV-JFH1 RNA in each knockdown cells at 96 h post-infection at an MOI of 0.05 were monitored by real-time LightCycler RT-PCR. (D) The levels of HCV core in the culture supernatants from the INI1 (INI1i) or DDX5 knockdown (DDX5i) RSc cells 96 h after inoculation of HCV-JFH1 were determined by ELISA. (E) The infectivity of HCV-JFH1 in the culture supernatants was determined by a focus-forming assay at 48 h post-infection. Virus titer is shown as ($x10^7$) FFU/ml. (F) WST-1 assay of each knockdown RSc cells at 96 h post-infection. (G) The HCV RNA replication level in INI1 and DDX5 knockdown OR6c JRN/3-5B cells was monitored by RL assay. (H) WST-1 assay of each knockdown OR6c JRN/3-5B cells. All results shown are means from three independent experiments.

4. Discussion

So far, the PML tumor suppressor protein, which forms PML-NBs, has been implicated in host antiviral defenses [6,7]. In fact, PML is induced by interferon after viral infection and suppresses some viral replication [6,7]. In contrast, PML-NBs are often disrupted or sequestered in the cytoplasm by infection with several DNA or RNA viruses to protect from the antiviral function of PML [6,7,23]. In case of HCV, Herzer et al. recently reported that the HCV core protein colocalizes with PML in PML-NBs and abrogates the PML function through interaction with PML isoform IV by over-expression studies [5]. However, we did not observe such colocalization of HCV core with PML and HCV did not affect the formation of PML-NBs in response to HCV-JFH1 infection (Fig. 3E). Interestingly, Watashi et al., previously demonstrated the HCV core modulates the retinoid signaling pathway through sequestration of

Sp110b, PML-related potent transcriptional corepressor of retinoic acid receptor, in the cytoplasm from nucleus [25].

In contrast, we have demonstrated that PML is required for infectious HCV production (Fig. 1). However, the molecular mechanism(s) how PML regulates HCV production yet remains unclear. At least, PML seems to be unrelated to the HCV RNA replication (Fig. 2). In this regard, several host factors including apolipoprotein E, components of ESCRT system, and PA28γ have been implicated in infectious HCV production [13,26,27]. Indeed, PA28γ, a proteasome activator, interacts with HCV core and affects nuclear retention and stability of the core protein. Importantly, PA28γ participates in the propagation of infectious HCV by regulation of degradation of the core protein [27]. Intriguingly, Zannini reported that PA28γ interacts with PML and Chk2 and affects PML-NBs number [28]. Accordingly, we demonstrated that ATM and Chk2, which phosphorylates PML and regulates the PML function, are involved in HCV life cycle [11]. In addition, other PML-related proteins such as INI1 and DDX5 seem to be involved in HCV production (Fig. 4). Indeed, INI1, also known as hSNF5, is incorporated into HIV-1 virion and is required for efficient HIV-1 production [29]. On the other hand, cytoplasmic PML may be involved in HCV production, since endoplasmic reticulum (ER) and lipid droplets are important cytoplasmic organelle for the HCV life cycle. In this regard, Giorgi et al. recently reported that cytoplasmic PML specifically enriches at ER [30], suggesting that cytoplasmic PML may be associated with HCV production. Altogether, the PML pathway seems to be involved in infectious HCV production.

Acknowledgments

We thank Drs. Didier Trono, Reuven Agami, Richard Iggo, Toshio Kitamura, Kenichi Abe and Apath LLC for the VSV-G-pseudotyped HIV-1-based vector system pCMVΔR8.91, pMDG2, pSUPER, pRDI292, Plat-E cells, pJRN/3-5B and pJFH1. We also thank Mr. Takashi Nakamura and Ms. Keiko Takeshita for their technical assistance. This work was supported by a Grant-in-Aid for Scientific Research (C) from the Japan Society for the Promotion of Science (JSPS), by a Grant-in-Aid for Research on Hepatitis from the Ministry of Health, Labor, and Welfare of Japan, and by the Viral Hepatitis Research Foundation of Japan. M. K. was supported by a Research Fellowship from JSPS for Young Scientists.

References

[1] N. Kato, Molecular virology of hepatitis C virus, Acta. Med. Okayama 55 (2001) 133–159.

[2] N. Kato, M. Hijikata, Y. Ootsuyama, et al., Molecular cloning of the human hepatitis C virus genome from Japanese patients with non-A, non-B hepatitis, Proc. Natl. Acad. Sci. USA 87 (1990) 9524–9528.

[3] Y. Miyanari, K. Atsuzawa, N. Usuda, et al., The lipid droplet is an important organelle for hepatitis C virus production, Nat. Cell Biol. 9 (2007) 1089–1097.

[4] D.R. McGivern, S.M. Lemon, Tumor suppressors, chromosomal instability, and hepatitis C virus-associated liver cancer, Annu. Rev. Pathol.: Mech. Dis. 4 (2009) 399–415.

[5] K. Herzer, S. Weyer, P.H. Krammer, et al., Hepatitis C virus core protein inhibits tumor suppressor protein promyelocytic leukemia function in human hepatoma cells, Cancer Res. 65 (2005) 10830–10837.

[6] R.D. Everett, M.K. Chelbi-Alix, PML and PML nuclear bodies: implications in antiviral defence, Biochimie 89 (2007) 819–830.

[7] E.L. Reineke, H.Y. Kao, Targeting promyelocytic leukemia protein: a means to regulating PML nuclear bodies, Intl. J. Biol. Sci. 5 (2009) 366–376.

[8] M. Kuroki, Y. Ariumi, M. Ikeda, et al., Arsenic trioxide inhibits hepatitis C virus RNA replication through modulation of the glutathione redox system and oxidative stress, J. Virol. 83 (2009) 2338–2348.

[9] T. Wakita, T. Pietschmann, T. Kato, et al., Production of infectious hepatitis C virus in tissue culture from a cloned viral genome, Nat. Med. 11 (2005) 791–796.

[10] Y. Ariumi, M. Kuroki, K. Abe, et al., DDX3 DEAD-box RNA helicase is required for hepatitis C virus RNA replication, J. Virol. 81 (2007) 13922–13926.

[11] Y. Ariumi, M. Kuroki, H. Dansako, et al., The DNA damage sensors ataxia-telangiectasia mutated kinase and checkpoint kinase 2 are required for hepatitis C virus RNA replication, J. Virol. 82 (2008) 9639–9646.

[12] Y. Ariumi, M. Kuroki, Y. Kushima, et al., Hepatitis C virus hijacks P-body and stress granule components around lipid droplets, J. Virol. 85 (2011) 6882–6892.

[13] Y. Ariumi, M. Kuroki, M. Maki, et al., The ESCRT system is required for hepatitis C virus production, PLoS One 6 (2011) e14517.

[14] M. Ikeda, K. Abe, H. Dansako, et al., Efficient replication of a full-length hepatitis C virus genome, strain O, in cell culture, and development of a luciferase reporter system, Biochem. Biophys. Res. Co. 329 (2005) 1350–1359.

[15] T.P. Brummelkamp, R. Bernard, R. Agami, A system for stable expression of short interfering RNAs in mammalian cells, Science 296 (2002) 550–553.

[16] A.J. Bridge, S. Pebernard, A. Ducraux, et al., Induction of an interferon response by RNAi vectors in mammalian cells, Nat. Genet. 34 (2003) 263–264.

[17] Y. Ariumi, F. Serhan, P. Turelli, et al., The integrase interactor 1 (INI1) proteins facilitate Tat-mediated human immunodeficiency virus type 1 transcription, Retrovirology 3 (2006) 47.

[18] L. Naldini, U. Blömer, P. Gallay, et al., In vivo gene delivery and stable transduction of nondividing cells by a lentiviral vector, Science 272 (1996) 263–267.

[19] R. Zufferey, D. Nagy, R.J. Mandel, et al., Multiply attenuated lentiviral vector achieves efficient gene delivery in vivo, Nat. Biotechnol. 15 (1997) 871–875.

[20] B.D. Lindenbach, M.J. Evans, A.J. Syder, et al., Complete replication of hepatitis C virus in cell culture, Science 309 (2005) 623–626.

[21] K. Ishii, K. Murakami, S.S. Hmwe, et al., Trans-encapsidation of hepatitis C virus subgenomic replicon RNA with viral structure proteins, Biochem. Biophys. Res. Co. 371 (2008) 446–450.

[22] E. Steinmann, C. Brohm, S. Kallis, et al., Efficient trans-encapsidation of hepatitis C virus RNAs into infectious virus-like particles, J. Virol. 82 (2008) 7034–7046.

[23] P. Turelli, V. Doucas, E. Craig, et al., Cytoplasmic recruitment of INI1 and PML on incoming HIV preintegration complexes: interference with early steps of viral replication, Mol. Cell 7 (2001) 1245–1254.

[24] G.J. Bates, S.M. Nicol, B.J. Wilson, et al., The DEAD box protein p68: a novel transcriptional coactivator of the p53 tumor suppressor, EMBO J. 24 (2005) 543–553.

[25] K. Watashi, M. Hijikata, A. Tagawa, et al., Modulation of retinoid signaling by a cytoplasmic viral protein via sequestration of Sp110b, a potent transcriptional corepressor of retinoic acid receptor, from the nucleus, Mol. Cell. Biol. 23 (2003) 7498–7509.

[26] K.S. Chang, J. Jiang, Z. Cai, et al., Human apolipoprotein E is required for infectivity and production of hepatitis C virus in cell culture, J. Virol. 81 (2007) 13783–13793.

[27] K. Moriishi, I. Shoji, Y. Mori, et al., Involvement of PA28γ in the propagation of hepatitis C virus, Hepatology 52 (2010) 411–420.

[28] L. Zannini, G. Buscemi, E. Fontanella, et al., REGγ/PA28γ proteasome activator interacts with PML and Chk2 and affects PML nuclear bodies number, Cell Cycle 8 (2009) 2399–2407.

[29] E. Yung, M. Sorin, A. Pal, et al., Inhibition of HIV-1 virion production by a transdominant mutant of integrase interactor 1, Nat. Med. 7 (2001) 920–926.

[30] C. Giorgi, K. Ito, H.K. Lin, et al., PML regulates apoptosis at endoplasmic reticulum by modulating calcium release, Science 330 (2010) 1247–1251.

HUMAN GENE THERAPY CLINICAL DEVELOPMENT 24:1–12 (XXX 2013)

DOI: 10.1089/humc.2013.066

Research Article

Long-Term Elimination of Hepatitis C Virus from Human Hepatocyte Chimeric Mice After Interferon-γ Gene Transfer

Yuki Takahashi,[1,*] Mitsuru Ando,[1,*] Makiya Nishikawa,[1] Nobuhiko Hiraga,[2] Michio Imamura,[2] Kazuaki Chayama,[2] and Yoshinobu Takakura[1]

Abstract

Chronic hepatitis C virus (HCV) infection is a leading cause of cirrhosis, liver failure, and hepatocellular carcinoma. Although the combination therapy employing pegylated interferon (IFN)-α and ribavirin is effective, this treatment is effective in only approximately 50% patients with genotype 1 HCV infection. IFN-γ is a potent anti-HCV agent that exhibits its antiviral action through a receptor distinct from that for IFN-α. Therefore, IFN-γ application might provide an alternative approach to IFN-α-based therapies. However, recombinant IFN-γ protein exhibits a poor pharmacokinetic property, that is, a very short half-life. It is our hypothesis that sustained IFN-γ serum concentrations produced by gene transfer could effectively eliminate HCV *in vivo*. We examined the *in vivo* antiviral activity in human hepatocyte chimeric mice infected with genotype 1b HCV at high HCV RNA titers (10^5–10^7 copies/ml). The human IFN-γ-expressing plasmid vector pCpG-huIFNγ exhibited prolonged transgene expression in mice compared with the plasmid vector pCMV-huIFNγ. Moreover, the gene transfer of pCpG-huIFNγ eliminated HCV from the liver of the chimeric mice for a sustained period. On the contrary, administration of pCMV-huIFNγ could not eliminate HCV. In conclusion, we found that a single pCpG-huIFNγ injection resulted in long-term elimination of HCV RNA in chimeric mice, providing, for the first time, direct evidence that chronic infection with high titer HCV *in vivo* can be treated by sustained IFN-γ treatment.

Introduction

Chronic hepatitis C virus (HCV) infection is a leading cause of cirrhosis, liver failure, and hepatocellular carcinoma (Niederau *et al.*, 1998). At present, the standard treatment for chronic HCV patients is a combination of pegylated interferon (IFN)-α and ribavirin (Manns *et al.*, 2001; Fried *et al.*, 2002). However, approximately only 50% of patients with genotype 1 HCV infection and a high viral load showed a sustained viral response, which is associated with resistance to IFN-α (Hofmann *et al.*, 2005; Chayama and Hayes, 2011). More recently, telaprevir, an HCV protease inhibitor, administered in combination with pegylated IFN and ribavirin has led to high rates of sustained virologic response. However, approximately 30% of patients with HCV genotype 1 infection did not respond to the combination treatment (Sherman *et al.*, 2011). Therefore, extensive efforts have been made to develop novel anti-HCV therapies that work via different mechanisms from that of IFN-α.

In vitro cell culture studies using HCV subgenomic replicon systems have demonstrated that IFN-γ (type II IFN) is a potent cytokine with anti-HCV activities (Cheney *et al.*, 2002; Frese *et al.*, 2002; Windisch *et al.*, 2005). The IFN-γ antiviral effects were stronger and more sustained than those of type I IFNs, such as IFN-α and IFN-β (Cheney *et al.*, 2002). Moreover, IFN-γ biological actions are mediated by a unique signal transduction pathway through cell surface receptors that are distinct from those of type I IFNs. Therefore, IFN-γ application could be an alternative therapeutic strategy for chronic HCV infection to overcome the drawbacks associated with present IFN-α-based therapies.

On the basis of the findings regarding IFN-γ anti-HCV activities, the therapeutic efficacy of IFN-γ was evaluated in chronic HCV patients. However, IFN-γ had little or no therapeutic effect in chronic HCV patients (Saez-Royuela *et al.*, 1991; Soza *et al.*, 2005). Although IFN-γ was repeatedly administered at high doses in these studies, the very short *in vivo* half-life of IFN-γ might have hampered its therapeutic

[1]Department of Biopharmaceutics and Drug Metabolism, Graduate School of Pharmaceutical Sciences, Kyoto University, Kyoto 606-8501, Japan.
[2]Department of Gastroenterology and Metabolism, Programs for Biomedical Research, Graduate School of Biomedical Science, Hiroshima University, Hiroshima 734-8551, Japan.
*These two authors contributed equally to this work.